NANO LETTERS

2007
Vol. 7, No. 12
3704−3708

Structures of D_{5d}-C_{80} and I_h-$Er_3N@C_{80}$ Fullerenes and Their Rotation Inside Carbon Nanotubes Demonstrated by Aberration-Corrected Electron Microscopy

Yuta Sato,* Kazu Suenaga,* Shingo Okubo, Toshiya Okazaki, and Sumio Iijima

Research Center for Advanced Carbon Materials, National Institute of Advanced Industrial Science and Technology (AIST), Tsukuba 305-8565, Japan

Received August 13, 2007; Revised Manuscript Received October 6, 2007

ABSTRACT

Time-dependent orientational changes of D_{5d}-C_{80} and I_h-$Er_3N@C_{80}$ fullerenes inside single-walled carbon nanotubes (SWNTs) were demonstrated by aberration-corrected transmission electron microscopy (TEM) at real atomic-level resolution. Detailed structure of the ellipsoidal D_{5d}-C_{80} fullerene, e.g., the pyrene-like tetracyclic component in its cylindrical body, was unambiguously identified by the TEM images. The Er−Er distances in I_h-$Er_3N@C_{80}$ were estimated to be 0.35 ± 0.03 nm, and the C_3 symmetry axis of the Er_3N cluster was suggested to agree with one of the S_6 axes of the spherical I_h-C_{80} cage. Our results indicate that atomic-resolution TEM enables the investigation of the orientations of individual molecules inside SWNTs in relation to the interactions of the molecules with the outer graphene walls.

One of the most attractive properties of carbon nanotubes (CNTs) is the ability to encapsulate various chemical species, such as inorganic crystals, organic molecules, and fullerenes.[1−4] The cylindrical spaces within CNTs are desirable environments to observe the structures and dynamic behavior of individual molecules by transmission electron microscopy (TEM). In the previous TEM studies on the molecules incorporated into single-walled CNTs (SWNTs), the nanotubes themselves have been regarded as almost contrast-less container materials due to the limited spatial resolution.[5−11] Recently, however, hexagonal networks of carbon atoms in SWNTs have been directly detected by aberration-corrected TEM, in which the spherical aberration coefficient (C_s) of the electron lens is reduced to nearly zero in order to improve the resolution.[12,13] This observation technique should also be able to visualize more detailed structures of encapsulated species inside SWNTs, such as individual fullerene molecules in so-called nanopeapods (fullerene-encapsulated nanotubes).

In our study, D_{5d}-C_{80} and I_h-$Er_3N@C_{80}$ fullerenes were incorporated into SWNTs for TEM observations. It has been recognized that the empty D_{5d}-C_{80} fullerene has a cylindrical body with hemispherical caps on both ends,[14] whereas the erbium nitride endohedral fullerene $Er_3N@C_{80}$ possesses a tetra-atomic Er_3N cluster inside the spherical I_h-C_{80} cage.[15,16] Only a limited number of experimental studies on the structures of these fullerene molecules have been reported up to now,[14−19] and their atomic-resolution images have never been obtained by TEM. These fullerenes are allowed to exhibit rotational motions inside SWNTs, which should be clearly detected by aberration-corrected TEM at an atomic-level resolution in the present study. Experimental procedures are described in the Supporting Information.

We first examined the advantage of aberration-corrected TEM in observation of individual D_{5d}-C_{80} fullerene cages by simulating their TEM images at large (uncorrected) and small (corrected) C_s values. The orientation of a D_{5d}-C_{80} fullerene is generally determined by parameters such as the tilt angle of its 5-fold axis with respect to the basal plane (e.g., a projection screen of TEM) and the rotation angle around this axis. D_{5d}-C_{80} cages at various tilt and rotation angles are illustrated schematically in Figure 1a, and their TEM images simulated at a large C_s value (0.5 mm) are shown in Figure 1b. The chromatic aberration coefficient (C_c) and defocus value (Δf) selected here are 1.1 mm and −40 nm, respectively. A bold ellipsoidal outline (or a circular one at a tilt angle of 90°) with a bright fringe is found for each D_{5d}-C_{80} cage. Only the tilt angle of the cage can be roughly estimated from the aspect ratio of this ellipsoidal outline. Rotation of the cage around the 5-fold axis does not significantly affect the contrast of the TEM image under the

* Corresponding authors. Tel.: +81-29-861-5694. Fax.:+81-29-861-4806. E-mail: yuta-sato@aist.go.jp (Y.S.); suenaga-kazu@aist.go.jp (K.S.).

10.1021/nl0720152 CCC: $37.00
Published on Web 11/10/2007

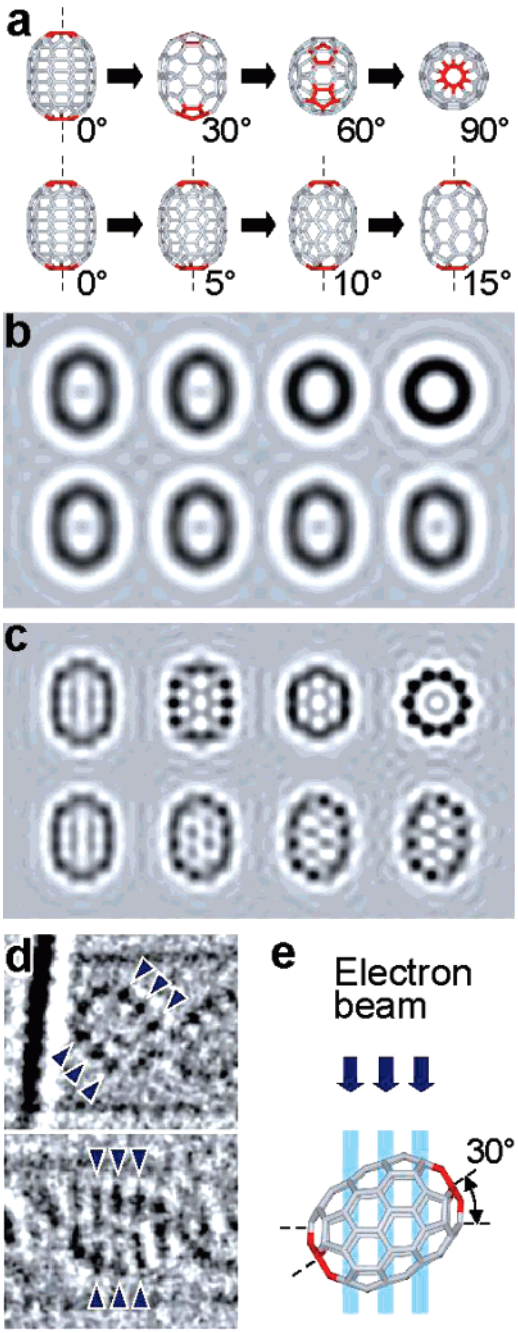

Figure 1. (a) Schematic illustration of the D_{5d}-C_{80} fullerene cages at various tilt and rotational angles (top and bottom rows, respectively). (b), (c) Simulated TEM images of the D_{5d}-C_{80} cages with C_s values of 0.5 mm (b) and 1 μm (c). (d) TEM images of D_{5d}-C_{80} cages at tilt angles of around 30° in SWNTs observed experimentally using the aberration-corrected microscope. (e) Schematic illustration of the D_{5d}-C_{80} cage tilted by 30°. A pair of five-membered rings penetrated by the 5-fold axis (dotted line) in each D_{5d}-C_{80} cage is colored red in (a) and (e). Characteristic contrast profiles found in (d) are indicated by blue triangles.

condition assumed here, in which the point resolution does not exceed 0.22 nm.

The D_{5d}-C_{80} cage should be visualized in significantly more detail using aberration-corrected TEM with a high resolution, pushed down to around 0.14 nm ($C_s = 1$ μm, $C_c = 1.1$ mm, $\Delta f = -5$ nm), as shown in Figure 1c. The TEM

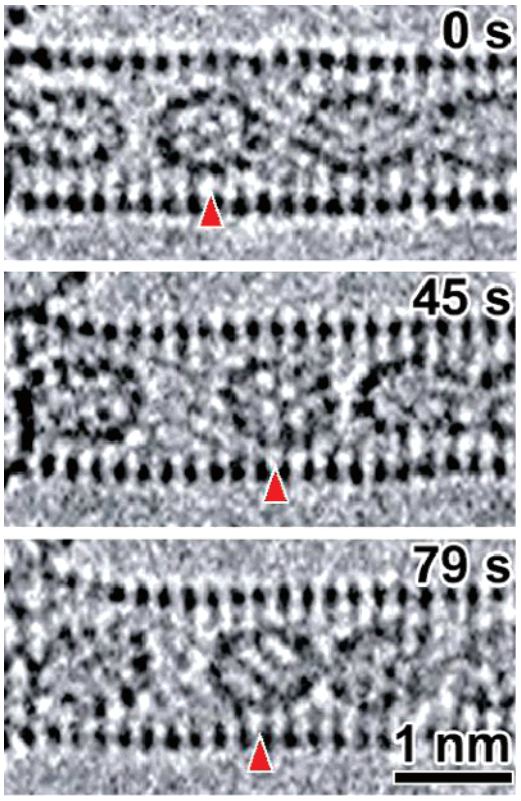

Figure 2. Sequential TEM images of the D_{5d}-C_{80} fullerene molecules inside the (18,1) SWNT observed experimentally using the aberration-corrected microscope. Orientational changes of the molecule marked with red triangles are clearly seen.

image exactly reflects both tilt and rotation angles of this fullerene cage, which enables the precise determination of the orientation.[20] The cylindrical body of this fullerene cage, in which the atomic arrangement is identical to that in a (5,5) SWNT, is most distinctly detected at a tilt angle of around 30°. The D_{5d}-C_{80} cage with this orientation yields a characteristic contrast profile with three dark dots on each sidewall in its TEM image, as also observed experimentally, shown in Figure 1d. These dark dots are ascribed to the projection of the zigzag chains parallel to the incident electron beam (Figure 1e).

The high spatial resolution and high detection ability of aberration-corrected TEM, as described above, suggest its significant advantage in monitoring the rotational motion of individual fullerene molecules. Figure 2 shows sequential TEM images of the D_{5d}-C_{80} fullerene cages aligned in the (18,1) SWNT. These fullerene cages inside the SWNT are more distinctly visualized than those attached to the outside,[21] since their motions are restricted in the confined space. The contrast of one of these cages (indicated by the red arrows) changes from frame to frame, which should be attributed to variation in its orientation.[22]

The images of encapsulated fullerene cages in Figure 2 inevitably overlap with the lattice image of the outer (18,1) SWNT, but the contrast of the latter image can be attenuated by processing via fast Fourier transformation (FFT) and inverse FFT (IFFT; see the Supporting Information, Figure S1). Some characteristic features in the original TEM images

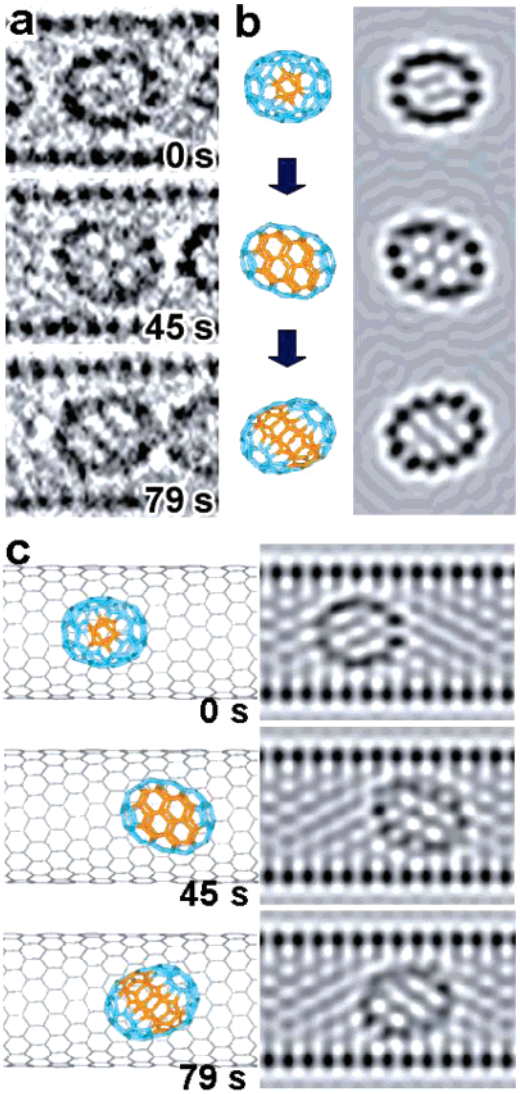

Figure 3. (a) FFT-processed TEM images of the D_{5d}-C_{80} fullerene focused in Figure 2. (b) Suggested orientations of the D_{5d}-C_{80} cage (left panel) and simulated TEM images (right panel). (c) Possible arrangement of the D_{5d}-C_{80} cage inside the (18,1) SWNT (left panels), and simulated TEM images that best agree with Figure 2 (right panels). Components in the D_{5d}-C_{80} cage that give characteristic contrast profiles in the TEM images are colored orange in (b) and (c).

of the marked cage are more clearly seen in the FFT-processed images in Figure 3a. The orientation of this fullerene cage can be determined based on these images, as shown in Figure 3b. The bright spot appearing at the center of the ellipsoidal cage at 0 s is ascribed to the staggered pair of pentagons on the top and bottom sides (orange-colored) that overlap with each other. In the second frame (45 s), this fullerene is oriented with one of its five mirror planes almost parallel to the projection screen. The four bright spots in this TEM image correspond to the pyrene-like tetracyclic components on both sides of the cage (orange-colored). In the third frame (79 s), a pair of parallel dark streaks from the anthracene-like tricyclic component on each side (orange-colored) are observed across the cage. Thus, the TEM images observed here strongly support the proposed structure of D_{5d}-C_{80}.[14]

The original TEM images in Figure 2 can be exactly simulated by taking into account the interference between the image of the encapsulated D_{5d}-C_{80} cage and that of the outer (18,1) SWNT. Simulated TEM images that best fit the observed images in Figure 2 are shown in Figure 3c, together with the schematic illustrations of the assumed models. Not only the orientation of the fullerene cage but also its relative position inside the SWNT should be carefully determined in order to reproduce the observed contrast profile. Figure S2 in the Supporting Information shows simulated TEM images of the D_{5d}-C_{80} cages that are identically oriented at slightly different positions inside the (18,1) SWNTs. The contrast in the simulated TEM images that agree with the observed images in Figure 2 is changed drastically when the fullerene cage is moved as slightly as 0.1 nm downward or upward along the nanotube axis. We can thus precisely determine both the orientation of each individual fullerene and its position inside a SWNT, based on the TEM images obtained at the corrected C_s value (see also the Supporting Information, Figure S3).

Aberration-corrected TEM was also applied to the metallofullerene I_h-$Er_3N@C_{80}$, in order to visualize its endohedral structure at a highly improved resolution. A TEM image of I_h-$Er_3N@C_{80}$ molecules aligned inside a (18,2) SWNT is shown in Figure 4a. Three I_h-$Er_3N@C_{80}$ molecules marked in this figure (**1**, **2**, and **3**) were observed to rotate without suffering significant damage by the electron beam, as shown in the sequential TEM images (Figure 4b). Three erbium atoms encapsulated in each fullerene cage are distinctly detected as dark dots, while the nitrogen atom bound to them does not give enough contrast. These dots are found to change their positions from frame to frame, due to the rotational motion of the I_h-$Er_3N@C_{80}$ molecule. The $Er_3N@C_{80}$ molecules **1**, **2**, and **3** at 28, 71, and 2 s, respectively, are almost identically oriented with respect to the incident electron beam. The Er−Er distances in these molecules are estimated to be 0.35 ± 0.03 nm based on the contrast profiles in the TEM images (Figure 4c), assuming that the Er_3N cluster possesses a 3-fold symmetry.[23]

The projected outline of each I_h-$Er_3N@C_{80}$ molecule in Figure 4b is almost round in shape, indicating the spherical structure of the I_h-C_{80} cage. According to the structures reported previously for the I_h isomers of the $M_3N@C_{80}$-type metallofullerenes such as $ErSc_2N@C_{80}$,[17] $Gd_3N@C_{80}$,[24] $Dy_3N@C_{80}$,[25] $Tb_3N@C_{80}$,[26] and $Lu_3N@C_{80}$,[27] the shortest Er−C distances in I_h-$Er_3N@C_{80}$ are expected to be 0.22−0.25 nm, and the Er−N distances are expected to be around 0.21 nm. Even such narrow gaps between the I_h-C_{80} cage and the Er atoms are distinctly resolved by aberration-corrected TEM. The contrast inside the I_h-C_{80} cages in the TEM images of $Er_3N@C_{80}$ is determined almost exclusively by the orientation of the Er_3N cluster with respect to the incident electron beam. The carbon-atom network in this fullerene cannot be faithfully imaged compared to the empty cages, due to disturbance by the encapsulated Er atoms with the much higher contrast.

Figure 5a shows the FFT-processed TEM images of the I_h-$Er_3N@C_{80}$ molecules **1** at 37 s and **3** at 2 s, in which the

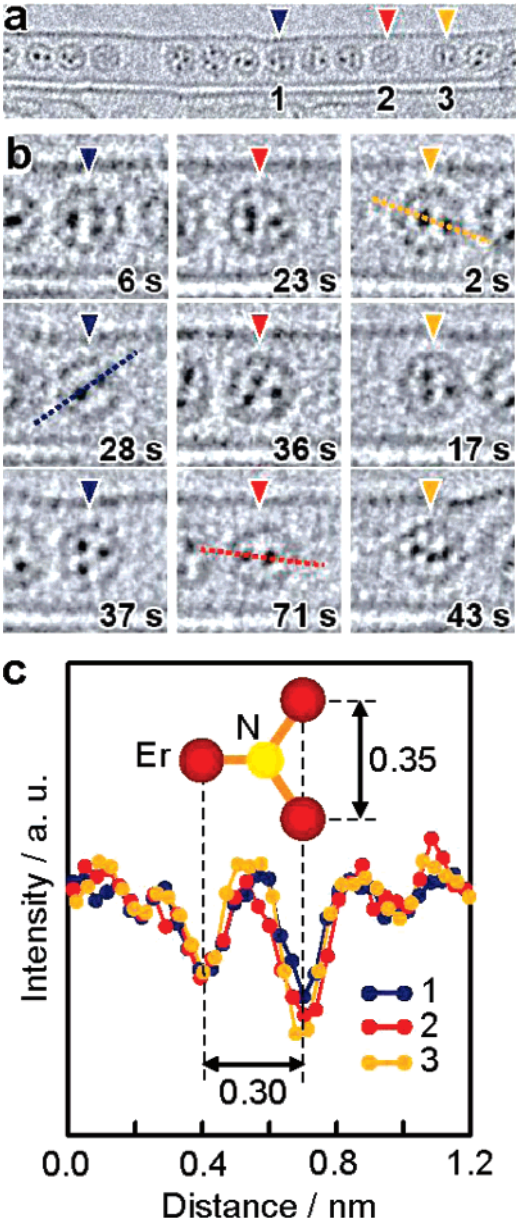

Figure 4. (a) A TEM image of the I_h-$Er_3N@C_{80}$ molecules aligned inside the (18,2) SWNT. (b) Sequential TEM images of the I_h-$Er_3N@C_{80}$ molecules **1**, **2**, and **3** (left, center and right panels, respectively) marked with triangles in (a). (c) Contrast profiles along the dotted lines in the TEM images of the I_h-$Er_3N@C_{80}$ molecules **1** (28 s), **2** (71 s) and **3** (2 s), from which the Er−Er distances are estimated to be 0.35 ± 0.03 nm.

contrast from the outer (18,2) SWNT is reduced. Characteristic dotted profiles are found on the outlines of the I_h-C_{80} cages in these images (indicated by red circles), enabling determination of the intracage orientation of the encapsulated Er_3N cluster. A possible structure of the I_h-$Er_3N@C_{80}$ molecule is illustrated in Figure 5b, together with the simulated TEM images that exactly reproduce the contrast of the observed images in Figure 5a. The TEM images of I_h-$Er_3N@C_{80}$ suggest that the C_3 symmetry axis of the Er_3N cluster agree with one of the S_6 axes of the I_h-C_{80} cage, as schematically shown in Figure 5c.

In summary, detailed structures of individual fullerene molecules, such as the cylindrical body of D_{5d}-C_{80} and

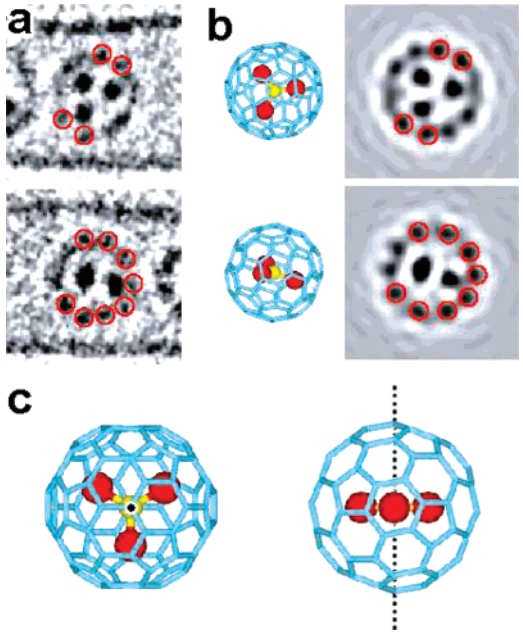

Figure 5. (a) FFT-processed TEM images of the I_h-$Er_3N@C_{80}$ molecules **1** at 37s (top panel) and **3** at 2 s (bottom panel). (b) Suggested orientations of the I_h-$Er_3N@C_{80}$ molecules (left panels) and simulated TEM images that best agree with (a) (right panels). (c) Schematic illustration of I_h-$Er_3N@C_{80}$ based on the intra-cage orientation of the Er_3N cluster deduced from the TEM images. The red and yellow balls in (b) and (c) correspond to the Er and N atoms, respectively. The black dot and dotted line in (c) show the 3-fold symmetry axis.

encapsulated Er atoms in I_h-$Er_3N@C_{80}$, were unambiguously visualized for the first time using aberration-corrected TEM. Both orientation and position of the D_{5d}-C_{80} cage were precisely determined with respect to the graphene structure of the outer SWNT, and the intracage orientation of the Er_3N cluster in I_h-$Er_3N@C_{80}$ could also be deduced from the TEM images. Even a slight orientational change or a slight translational motion of each fullerene cage encapsulated in a nanotube could be detected by aberration-corrected TEM. This observational technique should enable further discussion of the dynamic behavior of individual molecules inside SWNTs in relation to their atomic-level structures and to their interactions with outer graphene walls.

Acknowledgment. We gratefully acknowledge Prof. R. Hagiwara and Mr. T. Matsuno (Kyoto University) for their cooperation in characterization of materials. A part of this work was financially supported by the JST-CREST project.

Supporting Information Available: Experimental procedures and additional TEM images of D_{5d}-C_{80} fullerenes inside SWNTs. This material is available free of charge via the Internet at http://pubs.acs.org.

References

(1) Sloan, J.; Kirkland, A. I.; Hutchison, J. L.; Green, M. L. H. *Chem. Commun.* **2002**, *2002*, 1319.
(2) Monthioux, M. *Carbon* **2002**, *40*, 1809.
(3) Vostrowsky, O.; Hirsch, A. *Angew. Chem., Int. Ed.* **2004**, *43*, 2326.
(4) Kitaura, R.; Shinohara, H. *Chem. Asian J.* **2006**, *1*, 646.
(5) Smith, B. W.; Monthioux, M.; Luzzi, D. E. *Nature* **1998**, *396*, 323.

(6) Liu, Z.; Koshino, M.; Suenaga, K.; Mrzel, A.; Kataura, H.; Iijima, S. *Phys. Rev. Lett.* **2006**, *96*, 088304.
(7) Sato, Y.; Yumura, T.; Suenaga, K.; Moribe, H.; Nishide, D.; Ishida, M.; Shinohara, H.; Iijima, S. *Phys. Rev. B* **2006**, *73*, 193401.
(8) Sato, Y.; Yumura, T.; Suenaga, K.; Urita, K.; Kataura, H.; Kodama, T.; Shinohara, H.; Iijima, S. *Phys. Rev. B* **2006**, *73*, 233409.
(9) Koshino, M.; Tanaka, T.; Solin, N.; Suenaga, K.; Isobe, H.; Nakamura, E. *Science* **2007**, *316*, 853.
(10) Chamberlain, T. W.; Camenisch, A.; Champness, N. R.; Andrew, G.; Briggs, D.; Benjamin, S. C.; Ardavan, A.; Khlobystov, A. N. *J. Am. Chem. Soc.* **2007**, *129*, 8609.
(11) Liu, Z.; Yanagi, K.; Suenaga, K.; Kataura, H.; Iijima, S. *Nat. Nanotechnol.* **2007**, *2*, 422.
(12) Hirahara, K.; Saito, K.; Yamasaki, J.; Tanaka, N. *Nano Lett.* **2006**, *6*, 1778.
(13) Suenaga, K.; Wakabayashi, H.; Koshino, M.; Sato, Y.; Urita, K.; Iijima, S. *Nat. Nanotechnol.* **2007**, *2*, 358.
(14) Wang, C.-R.; Sugai, T.; Kai, T.; Tomiyama, T.; Shinohara, H. *Chem. Commun.* **2000**, *2000*, 557.
(15) Stevenson, S.; Rice, G.; Glass, T.; Harich, K.; Cromer, F.; Jordan, M. R.; Craft, J.; Hadju, E.; Bible, R.; Olmstead, M. M.; Maitra, K.; Fisher, A. J.; Balch, A. L.; Dorn, H. C. *Nature* **1999**, *401*, 55.
(16) Dunsch, L.; Yang, S. *Small* **2007**, *3*, 1298.
(17) Olmstead, M. M.; de Bettencourt-Dias, A.; Duchamp, J. C.; Stevenson, S.; Dorn, H. C.; Balch, A. L. *J. Am. Chem. Soc.* **2000**, *122*, 12220.
(18) Dunsch, L.; Krause, M.; Noack, J.;Georgi, P. *J. Phys. Chem. Solids* **2004**, *65*, 309.
(19) Krause, M.; Liu, X.; Wong, J.; Pichler, T.; Knupfer, M.; Dunsch, L. *J. Phys. Chem. A* **2005**, *109*, 7088.
(20) Under the present observation condition, both the tilt and the rotation of the cage are determined with accuracies of ±5° or better.
(21) Liu, Z.; Suenaga, K.; Iijima, S. *J. Am. Chem. Soc.* **2007**, *129*, 6666.
(22) This fullerene cage is not significantly damaged by the electron beam during the experiment, as indicated by fine agreement between observed and simulated TEM images in Figure 3.
(23) The planarity of the Er_3N cluster needs to be discussed in greater detail based on further analyses.
(24) Stevenson, S.; Phillips, J. P.; Reid, J. E.; Olmstead, M. M.; Rath, S. P.; Balch, A. L. *Chem. Commun.* **2004**, *2004*, 2814.
(25) Yang, S.; Troyanov, S. I.; Popov, A. A.; Krause, M.; Dunsch, L. *J. Am. Chem. Soc.* **2006**, *128*, 16733.
(26) Zuo, T.; Beavers, C. M.; Duchamp, J. C.; Campbell, A.; Dorn, H. C.; Olmstead, M. M.; Balch, A. L. *J. Am. Chem. Soc.* **2007**, *129*, 2035.
(27) Stevenson, S.; Lee, H. M.; Olmstead, M. M.; Kozikowski, C.; Stevenson, P.; Balch, A. L. *Chem. Eur. J.* **2002**, *8*, 4528.

NL0720152